Received September 3, 2017, accepted October 3, 2017, date of publication October 10, 2017, date of current version November 7, 2017.

Digital Object Identifier 10.1109/ACCESS.2017.2761846

Composite Sliding Mode Control of a Permanent Magnet Direct-Driven System For a Mining Scraper Conveyor

EN LU, WEI LI, XUEFENG YANG, AND SHAOYI XU
School of Mechatronic Engineering, China University of Mining and Technology, Xuzhou 221116, China

Corresponding author: Wei Li (cmeecumt512@yahoo.com)

This work was supported in part by the National Natural Science Foundation of China under Grant U1610111 and in part by the Project Funded by the Priority Academic Program Development of Jiangsu Higher Education Institutions.

ABSTRACT A composite sliding mode control based on the load characteristic of the permanent magnet direct-driven system is presented for a mining scraper conveyor. First, the mathematical model of a permanent magnet synchronous motor is established based on the coordinate transformation theory. Subsequently, the soft switching sliding mode observer (SS-SMO) is designed to observe the change of load torque in real time. The composite sliding mode speed controller of PMSM is designed on the basis of non-singular terminal sliding mode control, in which the observed load torque is used for feed-forward compensation. The chain characteristics of a scraper conveyor are described by the Kelvin-Vogit model, and the dynamic model of the overall scraper conveyor system is established with the distinct element method. Next, according to the coupling relationship between the permanent magnet direct-driven system and the scraper conveyor, the electromechanical coupling simulation model is established using the MATLAB/Simulink module. The simulation results demonstrate that the composite sliding mode controller of the permanent magnet direct-driven system can achieve smooth starting of the scraper conveyor, and the effectiveness of the designed controller is illustrated by comparing the controller with the related reference. In addition, the designed SS-SMO can estimate the load torque precisely, enhance system robustness and suppress the chattering of the control system caused by the load change.

INDEX TERMS Composite sliding mode control, PMSM, scraper conveyor, electromechanical coupling, load characteristic.

I. INTRODUCTION

The scraper conveyor is an important part of coal mining equipment, and its performance directly impacts the safety and efficiency of the entire mechanized working face [1]. The conveyor's composition is shown in Figure 1. A scraper conveyor will face various working conditions, such as rib spalling, abnormal load and blocked chain, and these conditions often lead to frequent overload and unplanned downtime due to the spontaneous complete drive failure. Additionally, the polygonal sprocket wheel, fluctuates dramatically and bending of the scraper chain will have severe impact on the scraper conveyor during runtime [2]. Thus, it can be seen that the scraper conveyor works in complex and poor working environment, and the traditional transmission mode adopting motor-reductor structure can easily experience failure [3].

With the continuous development of Field Oriented Control (FOC) and Direct Torque Control (DTC), the permanent magnet synchronous motor (PMSM) is widely used in the traditional transmission system which uses an AC induction motor, as in wind power generation [4],

FIGURE 1. Mining scraper conveyor.

equipment manufacturing [5], electric cars [6], marine propulsion [7], and so on. The concept of ''permanent magnet direct-drive'' has been developed over several years in related industries, but it is a relatively new topic in the coal mine production industry. A PMSM direct drive is adopted for a scraper conveyor, such that the reducer, and soft start device can be eliminated and ''near zero transmission'' is realized. Therefore, the advanced transmission mode of a scraper conveyor can effectively reduce the fault rate and improve the operating efficiency [8]. However, due to the complex and poor working environment, there is still a bottleneck for the application of PMSM in the scraper conveyor. Because the PMSM is connected directly to the scraper conveyor, the load characteristics will affect the stability of the speed control of the PMSM. Many scholars have proposed various methods to improve the control performances in systems with load disturbances and uncertainties. Baik *et al.* [9] proposed a non-linear controller using a feedback linearization technique and a boundary layer integral SMC technique. In the literature [10], the fuzzy sliding-mode approach was applied to a six-phase induction machine. A linear active disturbance rejection controller is applied for sensorless control of PMSM and the phase delay and speed chattering was clearly reduced [11]. Sira-Ramírez *et al.* [12] presented an active disturbance rejection control scheme for the angular velocity trajectory tracking task on a substantially perturbed and uncertain of PMSM.

Another efficient way of improving the disturbance rejection performance of a system in such cases is to introduce a feed forward compensation part into the controller in addition to the conventional anti-perturbation controller. Thus, the composite control method was applied to design the speed controller. A novel nonlinear speed control was proposed to improve the stability of the controller using the sliding mode control and disturbance compensation techniques [13]. Yang *et al.* developed a sliding-mode control (SMC) approach for systems with mismatched uncertainties via a non-linear disturbance observer (DOB) [14]. Wu *et al.* presented a linear active disturbance rejection controller for non-circular machining application, which is designed through an extended state observer to estimate and compensate the variant dynamics of the system, nonlinearly variable cutting load, and other uncertainties. In the literature [15], an extended sliding-mode observer of the load torque was proposed, of which the state variables were speed and load torque, in order to decrease the influence of the varying load torque in a PMSM control system.

In this paper, considering the abovementioned problem, the speed controller of the permanent magnet direct-driven system is addressed. First, an efficient disturbance estimation technique, namely, sliding mode observer, is introduced to estimate the disturbances load of the permanent magnet direct-driven system. To alleviate the chattering problem in the conventional sliding mode observer (SMO), a soft switching sliding mode observer (SS-SMO) is proposed, in which the traditional switching function is replaced with a boundary-layer-flexible sinusoidal saturation function. Hence, the chattering will be considerably reduced, while the disturbance rejection property of the closed-loop PMSM system can still be maintained. Subsequently, the non-singular terminal sliding mode control (NTSMC) is applied to design for the speed loop controller of the PMSM. To ensure that the closed-loop system possesses a good disturbance rejection property, the load observation value of the SS-SMO is fed to the input of the current regulator. Thus, a composite sliding mode controller (NTSMC+SS-SMO), using a combination of the sliding mode feedback part and disturbance compensation part based on SS-SMO, is developed. To verify the effect of the composite sliding mode controller, accurate simulation of the load characteristics of the permanent magnet direct-driven system is an important premise. The dynamic model of scraper conveyor reflects the relationship between the displacement, velocity and acceleration of the scraper chain and the dynamic load. Thus, the actual load curve of the permanent magnet direct-driven system can be simulated by the dynamic model of the scraper conveyor. Finally, simulation results and comparisons are given to show the effectiveness of the proposed method.

This study aims to investigate the composite sliding mode control of a permanent magnet direct-driven system for a mining scraper conveyor. The closed loop composite sliding mode controller of a permanent magnet direct-driven system is validated on the basis of the load characteristic which is obtained by the dynamic model of scraper conveyor. The paper is organized as follows: The design of the composite sliding mode controller for permanent magnet direct-driven system is explained in the following section. The 'Dynamic equations of scraper conveyor' section presents the dynamic model of the mining scraper conveyor based on the Kelvin-Vogit model. Subsequently, the MATLAB/Simulink model of the system is established according to the coupling relationship between the permanent magnet direct-driven system and the scraper conveyor in the section 'Electromechanical coupling modeling'. The simulation results of the composite sliding mode control of a permanent magnet direct-driven system for a mining scraper conveyor are given in the section 'Simulation and analysis of composite sliding mode controller'. A brief summary of the study is presented in the last section.

II. DESIGN OF COMPOSITE SLIDING MODE CONTROLLER

A. MATHEMATICAL MODEL OF THE PMSM

The stator voltage equation of the PMSM in the synchronous rotating coordinate (d-q) is shown as follows [16].

$$u_d = Ri_d + L_d \frac{di_d}{dt} - \omega_e L_q i_q \tag{1-a}$$

$$u_q = Ri_q + L_q \frac{di_q}{dt} + \omega_e L_d i_d + \omega_e \psi_f \tag{1-b}$$

where u_d and u_q are the d and q axes stator voltage components, i_d and i_q are the d and q axes stator current components, R is the stator resistance, L_d and L_q are the d and q axes inductances, ω_e is the rotor electrical speed, and ψ_f is the permanent magnet flux linkage, respectively.

The electromagnetic torque equation of the PMSM in the synchronous rotating coordinate (d-q) is shown as follows.

$$T_e = \frac{3}{2}p_n i_q[i_d(L_d - L_q) + \psi_f] \tag{2}$$

where p_n is the pole number of the PMSM.

According to the requirements of the permanent magnet direct-driven system for the mining scraper conveyor, a surface-mounted PMSM is selected as the driving motor. The control scheme of the PMSM is chosen as rotor flux orientation control ($i_d = 0$), and (2) can be simplified as follows.

$$T_e = \frac{3}{2}p_n i_q \psi_f \tag{3}$$

The mechanical motion equation of the PMSM is shown as follows.

$$T_e - T_L = B\omega_m + J\frac{d\omega_m}{dt} \tag{4}$$

where T_L is the load torque, B is the viscous friction coefficient, ω_m is the rotor mechanical speed and J is the rotational inertia , respectively.

B. DESIGN OF SS-SMO

According to the mechanical motion equation of the PMSM, the permanent magnet direct-driven system used in the direct drive mining scraper conveyor suffers from the effect of load torque change, which greatly increases the speed control instability. To reduce the effect of load sudden change on vector control systems, the SS-SMO is designed to observe the change of load torque of the PMSM in real time in this paper.

Because the switch frequency of the controller is much higher than the frequency of the load torque change, the load torque of the PMSM can be considered to be a slow variable in the control cycle. Therefore, the load can be assumed to be a constant value, namely, $\dot{T}_L = 0$. According to the (3) and (4), the following equation of state can be obtained

$$\begin{cases} \dot{\omega}_m = \frac{1}{J}(\frac{3p_n\psi_f}{2}i_q - T_L - B\omega_m) \\ \dot{T}_L = 0 \end{cases} \tag{5}$$

On the basis of (5), the following SMO of load torque can be constructed

$$\begin{cases} \dot{\hat{\omega}}_m = \frac{3p_n\psi_f}{2J}i_q - \frac{1}{J}\hat{T}_L - \frac{B}{J}\hat{\omega}_m + k_1 sgn(s) \\ \dot{\hat{T}}_L = k_2 sgn(s) \end{cases} \tag{6}$$

where $\hat{\omega}$ is the observation of electrical angular velocity, $\hat{T}_L$ is the observation of load torque, k_1 is the sliding mode gain of the load torque observer, k_2 is the feedback gain of the load torque observer, s is a sliding surface and $s = \hat{\omega} - \omega$.

To suppress the chattering problem in conventional SMO, this paper proposes a soft switching SMO for the load observation of the PMSM, in which the traditional switching function is replaced with a boundary-layer-flexible sinusoidal saturation function [17]. The boundary-layer-flexible sinusoidal saturation function sat(s) is shown as follows.

$$sat(s) = \begin{cases} sgn(s)\ |s| \geq \phi \\ \sin(\frac{\pi s}{2\phi})\ |s| < \phi \end{cases} \tag{7}$$

where ϕ is the boundary layer thickness. The curves of the conventional switching function and the sinusoidal saturation function are show in Figure 2.

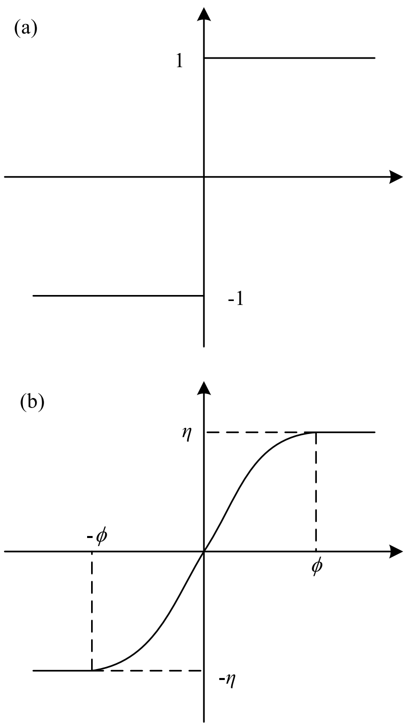

FIGURE 2. Curves of the conventional switching function and the sinusoidal saturation function (a: Conventional switching function, b: Boundary-layer-flexible sinusoidal saturation function).

Equation (6) is modified as follows:

$$\begin{cases} \dot{\hat{\omega}}_m = \frac{3p_n\psi_f}{2J}i_q - \frac{1}{J}\hat{T}_L - \frac{B}{J}\hat{\omega}_m + k_1 sat(s) \\ \dot{\hat{T}}_L = k_2 sat(s) \end{cases} \tag{8}$$

The observation error of the electric angular velocity is defined as $\tilde{\omega} = \hat{\omega}$-$\omega$, and the observation error of the load torque is defined as $\tilde{T}_L = \hat{T}_L - T_L$. According to the (5) and (6), the following error equation of state of SMO can be obtained

$$\begin{cases} \dot{\tilde{\omega}} = -\frac{1}{J}\tilde{T}_L - \frac{B}{J}\tilde{\omega} + k_1 sat(s) \\ \dot{\tilde{T}}_L = k_2\ sgn(s) \end{cases} \tag{9}$$

Proof: The following Lyapunov function candidate is considered [18]:

$$V = \frac{1}{2}s^2 \tag{10}$$

Differentiating V with respect to time, and it shows as follows:

$$\begin{aligned}\dot{V} &= s\dot{s}\\ &= s[k_1 sat(s) - \frac{1}{J}\tilde{T}_L - \frac{B}{J}\tilde{\omega}]\\ &= s[k_1 sat(s) - \frac{1}{J}\tilde{T}_L - \frac{B}{J}s]\\ &= -\frac{B}{J}s^2 + s[k_1 sat(s) - \frac{1}{J}\tilde{T}_L] \end{aligned} \tag{11}$$

where $B > 0, J > 0$. When $s[k_1 sat(s) - \frac{1}{J}\tilde{T}_L] \leq 0$, the SMO will satisfy the condition of asymptotic stability and it can be simplified as follows.

$$\begin{cases}\frac{1}{J}\tilde{T}_L + k_1 < 0, s < 0\\ \frac{1}{J}\tilde{T}_L - k_1 \geq 0, s \geq 0\end{cases} \tag{12}$$

Therefore, the range of the sliding mode gain can be obtained

$$k_1 \leq -\left|\frac{1}{J}\tilde{T}_L\right| \tag{13}$$

When the sliding mode load torque observer enters the steady state, the observation error of the electric angular velocity $\tilde{\omega} = \dot{\tilde{\omega}} = 0$, and the (9) can be simplified as:

$$\begin{cases}0 = -\frac{1}{J}\tilde{T}_L + k_1 sat(s)\\ \dot{\tilde{T}}_L = k_2 sgn(s)\end{cases} \tag{14}$$

Eq. (14) can be further simplified as.

$$\dot{\tilde{T}}_L - \frac{k_2}{k_1 J}\tilde{T}_L = 0 \tag{15}$$

According to the theory of stability, the stable condition of the (15) is $\frac{k_2}{k_1 J} < 0$. Due to the $k_1 < 0, J > 0$, the feedback gain of the SMO $k_2 > 0$ and the error of load torque is shown as [18]:

$$\tilde{T}_L = c_0 e^{\frac{k_2}{k_1 J}t} \tag{16}$$

where c0 is constant. The observation error of load torque $\hat{T}_L$ decreases with the increase of time t and reach to zero at last. Its approach speed is determined by the sliding mode gain k_1 and feedback gain k_2. If the appropriate parameter k_1 and k_2 are selected, $\dot{V} < 0$ can be guaranteed. The observation error of the electric angular velocity and load torque of PMSM is close to zero, and the vector control system of PMSM is stable

Finally, the principle diagram of the SS-SMO is shown in Figure 3.

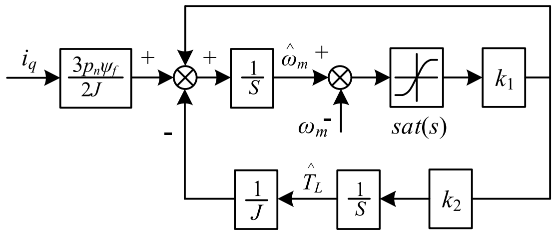

FIGURE 3. Principle diagram of the SS-SMO.

C. DESIGN OF COMPOSITE SLIDING MODE CONTROLLER

According to the (1), (3) and (4), the mathematical model of the surface-mounted PMSM can be expressed as follows based on rotor flux orientation control ($i_d = 0$).

$$\begin{cases}\frac{di_q}{dt} = \frac{1}{L_s}(-Ri_q - p_n\psi_f\omega_m + u_q)\\ \frac{d\omega_m}{dt} = \frac{1}{J}(-T_L + \frac{3p_n\psi_f}{2}i_q)\end{cases} \tag{17}$$

The state variables of the PMSM is defined as follows [19].

$$\begin{cases}\chi_1 = \omega_{ref} - \omega_m\\ \chi_2 = \dot{\chi}_1 = -\dot{\omega}_m\end{cases} \tag{18}$$

where ω_{ref} is the reference speed of the PMSM.

In the sliding mode control, the nonlinear function is introduced into the design of the sliding mode surface, which can make the tracking error of the sliding mode surface converge to zero within the limited time T, and the non-singular sliding mode surface is defined as follows.

$$s = \chi_1 + \frac{1}{\beta}\chi_2^{p/q} \tag{19}$$

where $\beta > 0$, p and q ($p > q$) are positive odd numbers.

The exponential reaching law function is shown as follows.

$$slaw = -\varepsilon sgn(s) - qs\varepsilon > 0, q > 0 \tag{20}$$

Taking the derivative of the sliding surface $\dot{s}$, the (20) is substituted into it, then (21) is obtained as follows.

$$\dot{s} = \dot{\chi}_1 + \frac{p}{q\beta}\chi_2^{p/q-1}\cdot\dot{\chi}_2 = \chi_2 + \frac{p}{q\beta}\chi_2^{p/q-1}\cdot\dot{\chi}_2 = slaw \tag{21}$$

The expression of the controller is shown as follows.

$$\dot{i}_q = \frac{2J}{3p_n\psi_f}\left(\beta\frac{q}{p}\chi_2^{2-p/q} + \varepsilon sgn(s) + qs\right) \tag{22}$$

Thus, the reference current of the q axis is expressed as follows.

$$i_q = \frac{2J}{3p_n\psi_f}\int_0^t\left(\beta\frac{q}{p}\chi_2^{2-p/q} + \varepsilon sgn(s) + qs\right)dt \tag{23}$$

Proof: In order to analyze stability of the NTSMC, the following Lyapunov function is considered.

$$V = \frac{1}{2}s^2 \tag{24}$$

Differentiating V with respect to time, and it shows as follows:

$$\begin{aligned}\dot{V} &= s\dot{s}\\ &= s(\chi_2 + \frac{p}{q\beta}\chi_2^{p/q-1}\cdot\dot{\chi}_2)\\ &= s[\frac{p}{q\beta}\chi_2^{p/q-1}(-\varepsilon sgn(s) - qs)]\\ &= \frac{p}{q\beta}\chi_2^{p/q-1}(-\varepsilon|s| - qs^2)\end{aligned} \tag{25}$$

Due to the $\varepsilon > 0$, $\beta > 0$, p and q $(p > q)$ are positive odd numbers, the (25) can be simplified as:

$$s\dot{s} = \frac{p}{q\beta}\chi_2^{p/q-1}(-\varepsilon\,|s| - qs^2) \leq 0 \tag{26}$$

Therefore, the desigened NTSMC is asymptotically stable.

The load observation value of the SS-SMO is fed to the input of the current regulator, and the disturbance feed forward compensation is marked as i_q'. Combined with the (23), the final reference current of the q axis is expressed as follows.

$$\begin{aligned} i_q^* &= i_q + i_q' \\ &= \frac{2J}{3p_n\psi_f}\int_0^t\left(\beta\frac{q}{p}\chi_2^{2-p/q} + \varepsilon sgn(s) + qs\right)dt + k_t\hat{T}_L \end{aligned} \tag{27}$$

where k_t is the feed forward gain for load disturbance compensation, and $k_t > 0$.

The real-time load torque of the PMSM is identified by the SS-SMO, and the load observation value of the SS-SMO is fed to the input of the current regulator. The influence of the sudden load on the speed control of the PMSM of the scraper conveyor can be overcome effectively and reduce the speed fluctuation of the PMSM. The composite sliding mode control scheme of the PMSM is shown in Figure 4.

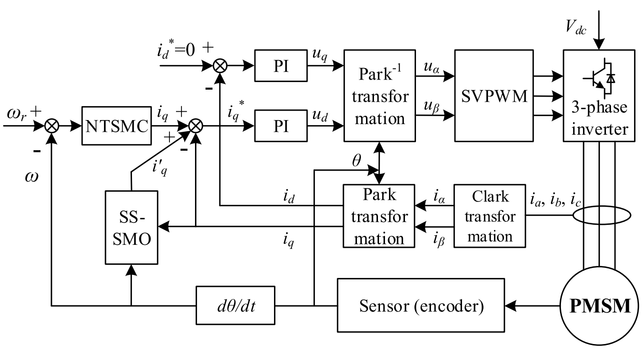

FIGURE 4. Composite sliding mode control scheme of PMSM.

III. DYNAMIC EQUATIONS OF SCRAPER CONVEYOR

The chain characteristics of the scraper conveyor are described by the Kelvin-Vogit model, and the model is shown in Figure 5.

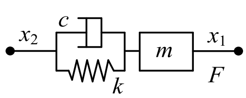

FIGURE 5. Kelvin-Vogit model of chain.

The tension can be expressed as the following form.

$$F = k(x_1 - x_2) + c(\dot{x}_1 - \dot{x}_2) \tag{28}$$

where k the stiffness coefficient of the chain, and c is the viscous damping coefficient of chain.

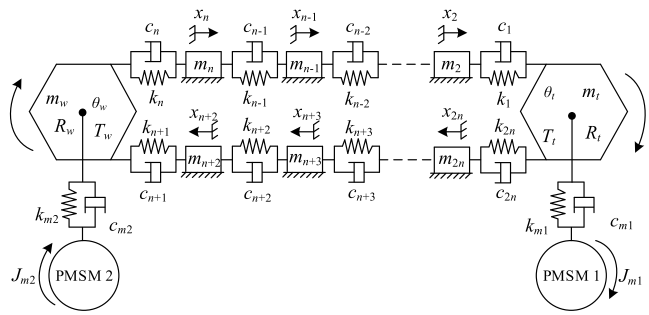

FIGURE 6. Discrete element model of the scraper conveyor.

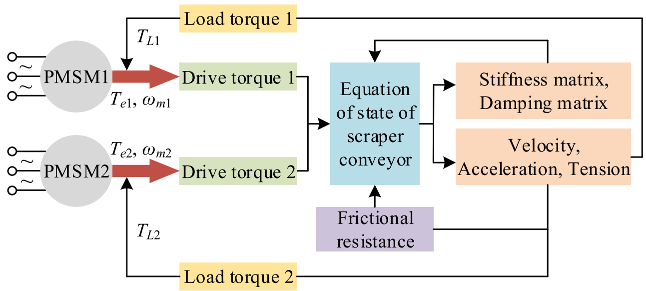

FIGURE 7. Schematic block diagram of the electromechanical coupling model.

According to distinct element method, the chain of the scraper conveyor is divided into $2n$ discrete mass systems and is shown in Figure 6.

The dynamic equation of the chain elements can be expressed as follows [20].

$$F_{i-1} - F_i - f_i = m_i\ddot{x}_i \tag{29}$$

where F_{i-1} is the tension of the i-1$^{\text{th}}$ element, F_i is the tension of thei^{th} element, f_i is the frictional resistance of the i^{th} element, m_i is the lumped mass of the i^{th} element, $\ddot{x}_i$ is the acceleration of the i^{th} element.

The resistances of the scraper conveyor are changed with time, and they can be described by the following formula [1].

$$f_i = \begin{cases} F_{i-1} & (v \approx 0, F_{i-1} - F_i \leq f_s) \\ f_d & (v > 0, x > 0) \end{cases} \tag{30}$$

where f_s is the static friction force of the chain elements, f_d is the dynamic friction force of the chain elements.

The movement forming the head and tail element of the scraper conveyor is rotation and the dynamic equations can be expressed as follows.

$$\begin{cases} T_t + (F_{2n} - F_1 - f_t)R_t = \dfrac{1}{2}m_tR_t^2\ddot{\theta}_t \\ T_w + (F_n - F_{n+1} - f_w)R_w = \dfrac{1}{2}m_wR_w^2\ddot{\theta}_w \end{cases} \tag{31}$$

where T_t is the drive torque of the head element, T_w is the drive torque of the tail element, R_t is the radius of the sprocket wheel of the head element, R_w is the radius of the sprocket

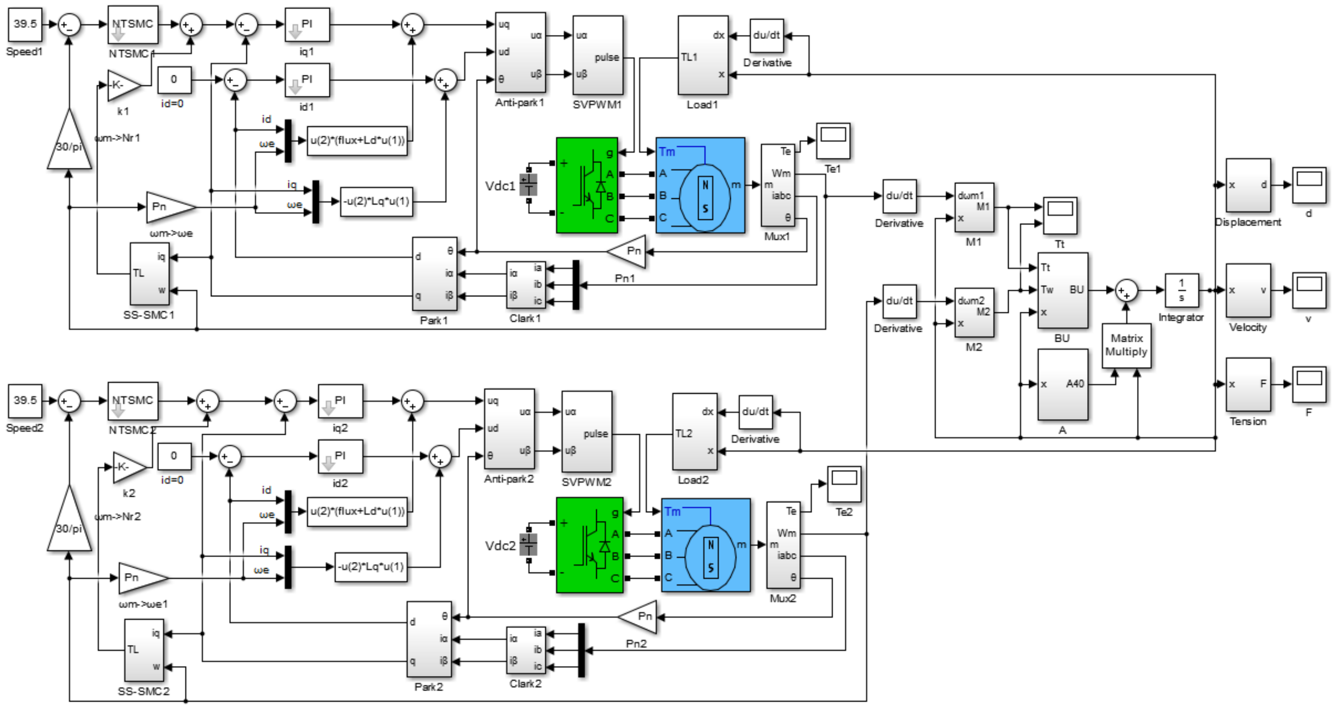

FIGURE 8. Electromechanical coupling model of the mining scraper conveyor.

wheel of the tail element, m_t is the mass of the sprocket wheel of the head element, m_w is the mass of the sprocket wheel of the tail element, $\ddot{\theta}_t$ is the angular acceleration of the sprocket wheel of the head element, $\ddot{\theta}_w$ is the angular acceleration of the sprocket wheel of the head element.

Based on (29), (30) and (31), the dynamic equations of scraper conveyor can be obtained as follows [22].

$$\begin{cases} \frac{1}{2}m_t R_t \ddot{\theta}_t + F_1 - F_{2n} = \frac{T_t}{R_t} - f_t \\ m_2\ddot{x}_2 + F_2 - F_1 = -f_2 \\ \quad\cdots\cdots \\ m_n\ddot{x}_n + F_n - F_{n-1} = -f_n \\ \frac{1}{2}m_w R_w \ddot{\theta}_w + F_{n+1} - F_n = \frac{T_w}{R_w} - f_w \\ \quad\cdots\cdots \\ m_{2n}\ddot{x}_{2n} + F_{2n} - F_{2n-1} = -f_{2n} \end{cases} \tag{32}$$

Equation (32) can be simplified as follows.

$$\boldsymbol{M}\ddot{x} + \boldsymbol{C}\dot{x} + \boldsymbol{K}x + \boldsymbol{W} = \boldsymbol{F} \tag{33}$$

where $\boldsymbol{M}$ is the mass matrix, $\boldsymbol{C}$ is the damping matrix, $\boldsymbol{K}$ is the stiffness matrix, $\boldsymbol{W}$ is the resistance matrix, $\boldsymbol{F}$ is the external force matrix.

In this equation, the state vector is defined as $V = [x_t, x_2, \cdots, x_w, x_{n+2}, \cdots x_{2n}, \dot{x}_t, \dot{x}_2, \cdots, \dot{x}_w, \dot{x}_{n+2}, \cdots \dot{x}_{2n}]$, and the equation of state is shown as follows.

$$\begin{cases} \dot{\boldsymbol{V}} = \boldsymbol{A}\boldsymbol{V} + \boldsymbol{B}\boldsymbol{U} \\ \boldsymbol{y} = \boldsymbol{C}\boldsymbol{V} + \boldsymbol{D}\boldsymbol{U} \end{cases} \tag{34}$$

where $\boldsymbol{A} = \begin{bmatrix} 0 & \boldsymbol{I} \\ -\boldsymbol{M}^{-1}\boldsymbol{K} & 0 \end{bmatrix}$, $\boldsymbol{B} = \begin{bmatrix} 0 \\ \boldsymbol{M}^{-1}\boldsymbol{F} \end{bmatrix}$, $\boldsymbol{C} = \begin{bmatrix} 1 & 0 & 0 \\ 0 & \ddots & 0 \\ 0 & 0 & 1 \end{bmatrix}$, $\boldsymbol{D} = [0]$.

IV. ELECTROMECHANICAL COUPLING MODELING

The correlation between the permanent magnet direct-driven system and scraper conveyor is the first premise and guarantee of the building electromechanical coupling model. According to the (20), the load of the permanent magnet direct-driven system can be expressed as follows.

$$\begin{cases} T_{L1} = \frac{1}{2}m_t R_t^2 \ddot{\theta}_t - (F_{2n} - F_1 - f_t)R_t \\ T_{L2} = \frac{1}{2}m_w R_w^2 \ddot{\theta}_w - (F_n - F_{n+1} - f_w)R_w \end{cases} \tag{35}$$

Then, the schematic block diagram of the electromechanical coupling model is shown in Figure 7.

The simulation parameters of the PMSM and scraper conveyor are shown in Table 1.

According to the schematic block diagram of the electromechanical coupling model, the entire simulation model of the mining scraper conveyor is established by

TABLE 1. Simulation parameters of the permanent magnet drive scraper conveyor.

Mining scraper conveyor	Transmission capacity Q (t/h)	2000
	Length L_s (m)	200
	Chain velocity Vs (m/s)	1.2
	Radius of sprocket wheel R (m)	0.29
	Middle trough Length × Width × Height (mm)	1500×1000×362
	Chain specification (mm)	42×156
	Center distance of chain (mm)	260
PMSM	Rated power P_N (kW)	560kW
	Rated voltage V_N (V)	1140
	Rated current I_N (A)	314
	Rated speed n_N (r/min)	40
	Rated torque T_N (kN.m)	144.54

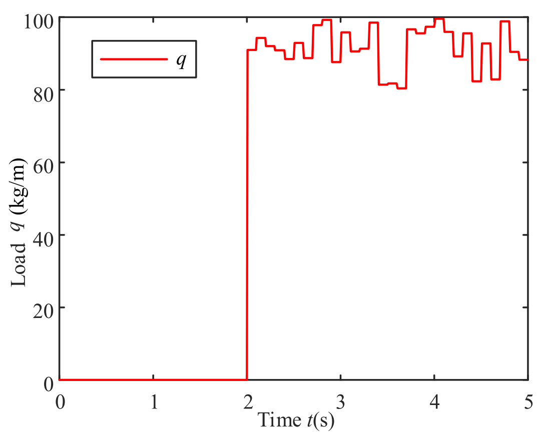

FIGURE 9. Load of unit length of scraper conveyor.

MATLAB/Simulink and simulation parameters and is shown in Figure 8.

V. SIMULATION AND ANALYSIS OF COMPOSITE SLIDING MODE CONTROLLER

According to the chain velocity and the radius of the polygonal sprocket wheel, the speed of the PMSM is obtained, and the value is 39.5 r/min. Figure 9 is the load of unit length of the scraper conveyor, the scraper conveyor worked under the no load condition in the 0 to 2 s, and the scraper conveyor worked under the random load condition in the range of 2 to 5 s which is in the range of 80%∼100% full load.

Based on the composite sliding mode controller of the permanent magnet direct-driven system, the simulation curves of the scraper conveyor under random load condition are shown in Figure 10. Figure 10(a) is the 3D plot of the chain velocity change of the scraper conveyor. Figure 10(b) is the chain velocity of the scraper conveyor on the location of $x = 100$ m

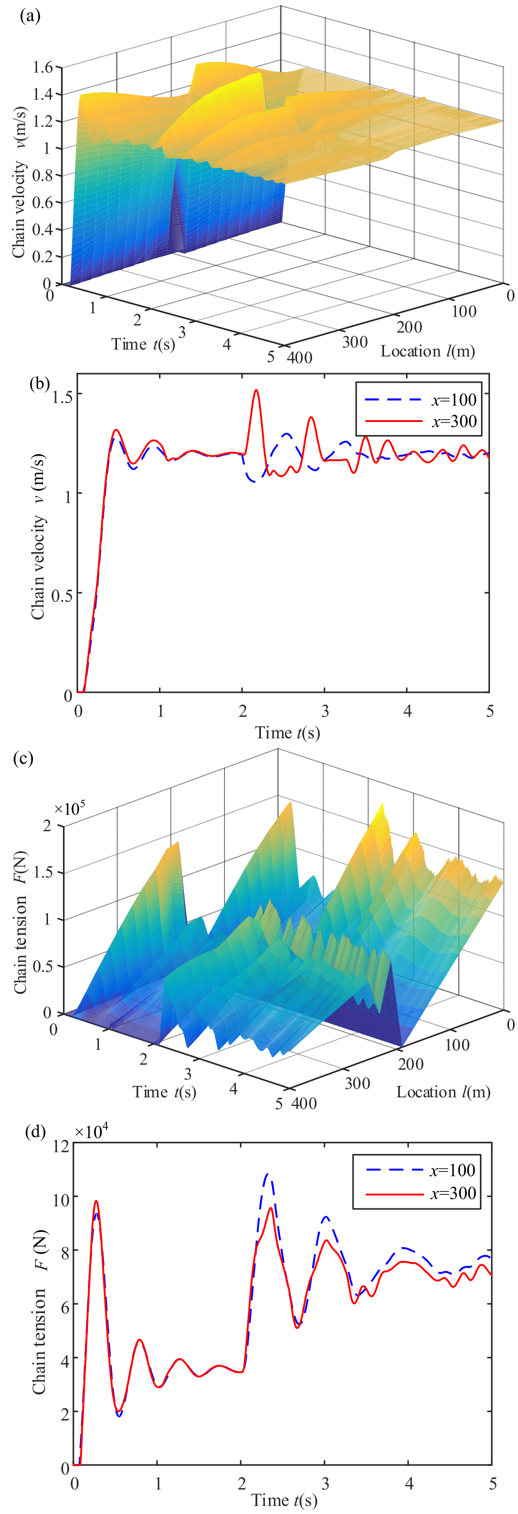

FIGURE 10. Simulation curves of scraper conveyor under random load condition (a: Chain velocity of scraper conveyor, b: Chain velocity of scraper conveyor on the location of $x = 100$ m and $x = 300$ m, c: Chain tension of scraper conveyor, d: Chain tension of scraper conveyor on the location of $x = 100$ m and $x = 300$ m).

and $x = 300$ m, the chain velocity shows fluctuations due to the influence of the random load. Figure 10(c) is the 3D plot of the chain tension change of the scraper conveyor.

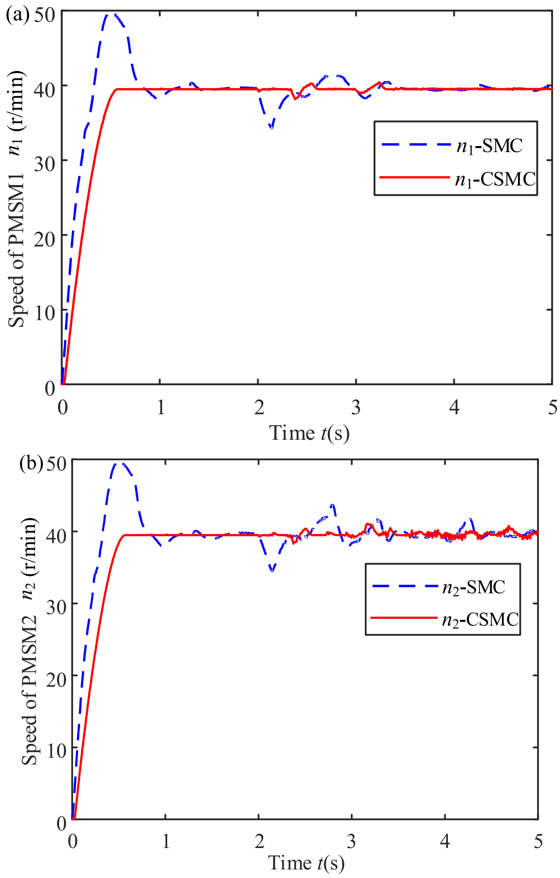

FIGURE 11. Simulation curves of the sliding mode controller and composite sliding mode controller (a: Speed of PMSM1, b: Speed of PMSM2).

Figure 10(d) is the chain tension of the scraper conveyor on the location of $x = 100$ m and $x = 300$ m, the chain tension also shows fluctuations due to the influence of the random load. Furthermore, the simulation curves of the scraper conveyor show that the composite sliding mode controller can realize smooth starting and stable operation of the mining scraper conveyor under random load conditions.

The effectiveness of the composite sliding mode controller is illustrated by comparing the controller with literature [15], and the results of the simulation experiment are shown in Figure 11. Figure 11(a) shows the speed curves of PMSM1. Compared with the general sliding mode controller in the literature [15], the designed controller has a smaller overshoot and better robust stability. The speed curves of PMSM2 also illustrate the excellent performance of the designed controller which are shown in Figure 11(b).

The simulation curves of the non-singular terminal sliding mode controller (NTSMC) and composite sliding mode controller (NTSMC+SS-SMO) of the permanent magnet direct-driven system are given to explain the effectiveness of the SS-SMO and are shown in Figure 12. Figure 12(a) shows the speed curves of PMSM1. Compared with the non-singular terminal sliding mode controller, the effect of random load on the control system can be reduced effectively by the composite sliding mode controller which combines the non-singular terminal sliding mode controller and the SS-SMO. The speed curves of PMSM2 also illustrate this point, which are shown

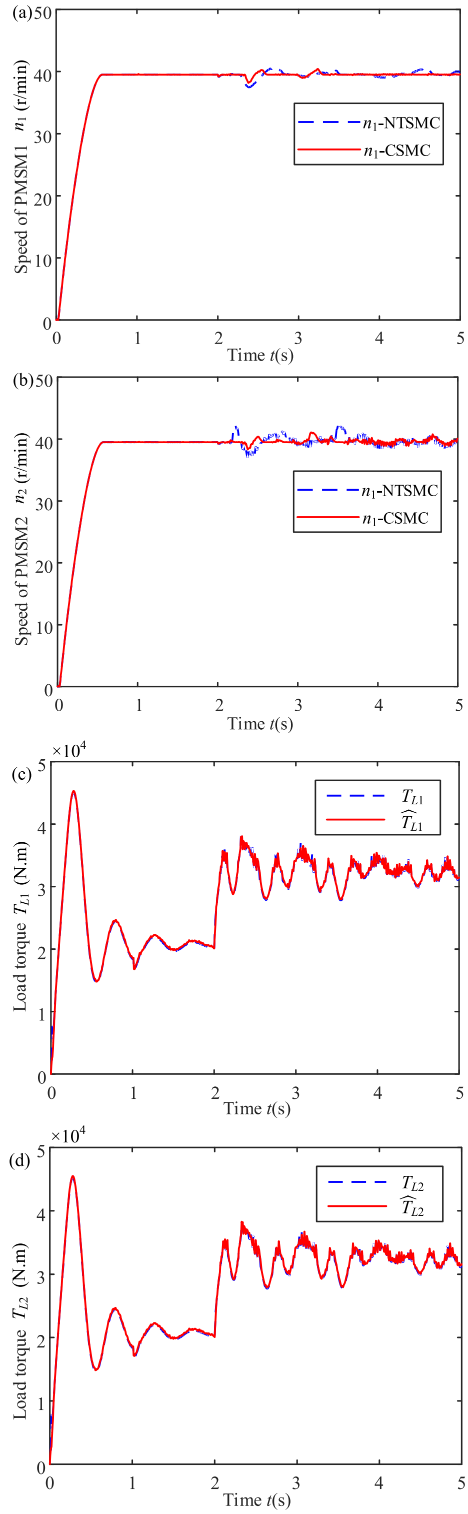

FIGURE 12. Simulation curves of the non-singular terminal sliding mode controller and composite sliding mode controller (a: Speed of PMSM1, b: Speed of PMSM2, c: Load torque of SS-SMO1, d: Load torque of SS-SMO2).

in Figure 12(b). Figure 12(c) shows the simulation curves of the actual load torque and the observation value of the SS-SMO1 and shows that the SS-SMO1 can accurately observe the actual load torque of the PMSM1. Figure 12(d) supports this finding.

VI. CONCLUSIONS

In this study, the composite sliding mode control of the permanent magnet direct-driven system for the mining scraper conveyor is analyzed based on the load characteristic. The composite sliding mode controller is designed on the basis of the SS-SMO and NTSMC. The electromechanical coupling model between the permanent magnet direct-driven system and the scraper conveyor is established based on the mathematical model of the PMSM with the dynamic model of the scraper conveyor. Finally, the performance of the composite sliding mode controller is investigated through numerical simulations.

The analysis of the starting condition under random load shows that the composite sliding mode speed controller can realize smooth starting and stable operation of the scraper conveyor, the random load affects the stability of the chain velocity and chain tension, and the change curves respond directly to the random load characteristics. Compared the designed controller with related reference, we determine that the composite sliding mode controller has excellent performance, smaller overshoot and better robust stability. Compared with the NTSMC, the effect of random load on the control system can be reduced effectively by the composite sliding mode controller, in which the observed load torque of the SS-SMO is used for feed-forward compensation. The designed SS-SMO can accurately observe the load torque change of the permanent magnet direct-driven system in real time.

REFERENCES

[1] G. F. Wang, "New development of longwall mining equipment based on automation and intelligent technology for thin seam coal," *J. Coal Sci., Eng.*, vol. 19, no. 1, pp. 97–103, 2013.

[2] P. Sobota, "Determination of the friction work of a link chain interworking with a sprocket drum," *Arch. Mining Sci.*, vol. 58, no. 3, pp. 805–822, 2013.

[3] S. H. Ma, "Control technology and application for driving device of flight conveyer," *Explosion-Proof Electr. Mach.*, vol. 45, no. 2, pp. 30–32, 2010.

[4] L. Y. Shao *et al.*, "Influence of rotor-pole number on electromagnetic performance in 12-phase redundant switched flux permanent magnet machines for wind power generation," *IEEE Trans. Ind. Appl.*, vol. 53, no. 4, pp. 3305–3316, Jul./Aug. 2017.

[5] J. Nerg, M. Rilla, V. Ruuskanen, J. Pyrhonen, and S. Ruotsalainen, "Direct-driven interior magnet permanent-magnet synchronous motors for a full electric sports car," *IEEE Trans. Ind. Electron.*, vol. 61, no. 8, pp. 4286–4294, Aug. 2014.

[6] W. Q. Lu *et al.*, "Double servo synchronization drive control strategy for the main slide carriage of broaching machine based on disturbance compensation algorithm," *J. Mech. Eng.*, vol. 49, no. 21, pp. 31–37, 2013.

[7] H. Bai, J. Zhu, and J. Qin, "Performance study of three-phase fault-tolerant permanent magnet motor drive for marine propulsion system based on structure design," *J. Ship Res.*, vol. 61, no. 1, pp. 23–34, 2016.

[8] J. S. Chen, J. G. Liu, and Y. Zhang, "New vector control of the permanent magnet synchronous motor," *J. Xidian Univ.*, vol. 41, no. 4, pp. 179–185, 2014.

[9] I.-C. Baik, K.-H. Kim, and M.-J. Youn, "Robust nonlinear speed control of PM synchronous motor using boundary layer integral sliding mode control technique," *IEEE Trans. Control Syst. Technol.*, vol. 8, no. 1, pp. 47–54, Jan. 2000.

[10] M. A. Fnaiech, F. Betin, G.-A. Capolino, and F. Fnaiech, "Fuzzy logic and sliding-mode controls applied to six-phase induction machine with open phases," *IEEE Trans. Ind. Electron.*, vol. 57, no. 1, pp. 354–364, Jan. 2010.

[11] B. Du, S. Wu, S. Han, and S. Cui, "Application of linear active disturbance rejection controller for sensorless control of internal permanent-magnet synchronous motor," *IEEE Trans. Ind. Electron.*, vol. 63, no. 5, pp. 3019–3027, May 2016.

[12] H. Sira-Ramírez, J. Linares-Flores, C. García-Rodríguez, and M. A. Contreras-Ordaz, "On the control of the permanent magnet synchronous motor: An active disturbance rejection control approach," *IEEE Trans. Control Syst. Technol.*, vol. 22, no. 5, pp. 2056–2063, Sep. 2014.

[13] X. Zhang, L. Sun, K. Zhao, and L. Sun, "Nonlinear speed control for PMSM system using sliding-mode control and disturbance compensation techniques," *IEEE Trans. Power Electron.*, vol. 28, no. 3, pp. 1358–1365, Mar. 2013.

[14] J. Yang, S. Li, and X. Yu, "Sliding-mode control for systems with mismatched uncertainties via a disturbance observer," *IEEE Trans. Ind. Electron.*, vol. 60, no. 1, pp. 160–169, Jan. 2013.

[15] X. G. Zhang, L. Sun, and K. Zhao, "Sliding mode control of PMSM based on a novel load torque sliding mode observer," *Chin. Soc. Elect. Eng.*, vol. 32, no. 3, pp. 111–116, 2012.

[16] J.-J. Ren, Y.-C. Liu, N. Wang, and S.-Y. Liu, "Sensorless control of ship propulsion interior permanent magnet synchronous motor based on a new sliding mode observer," *ISA Trans.*, vol. 54, no. 2, pp. 15–26, 2015.

[17] X. Q. Lu, L. Heyun, and F. Yi, "Soft switching sliding mode observer for PMSM sensorless control," *Trans. China Electrotech. Soc.*, vol. 30, no. 2, pp. 106–113, 2015.

[18] N. Wang and X. Y. Liu, "Load disturbance rejection based dualslidingmode control of permanentmagnet synchronous motors," *J. Dalian Maritime Univ.*, vol. 42, no. 2, pp. 75–82, 2016.

[19] L. Qi and H. Shi, "Adaptive position tracking control of permanent magnet synchronous motor based on RBF fast terminal sliding mode control," *Neurocomputing*, vol. 115, pp. 23–30, Sep. 2013.

[20] B. Y. He, Y. Sun, R. Nie, and G. Li, "Dynamic behavior analysis on the ring chain transmission system of an armoured face conveyor," *J. Mech. Eng.*, vol. 48, no. 17, pp. 50–56, 2012.

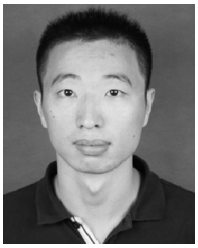

EN LU was born in 1990. He received the B.E. and M.E. degrees from the School of Mechatronic Engineering, China University of Mining and Technology, Xuzhou, China, in 2013 and 2015, respectively, where he is currently pursuing the Ph.D. degree. His research interests include dynamic analysis and control of PMSM.

WEI LI was born in 1964. He received the B.E. degree from the School of automation engineer, University of Electronic Science and Technology of China, Chengdu, China, in 1986, and the M.E. and Ph.D. degrees from the China University of Mining and Technology, Xuzhou, China, in 1989 and 2004, respectively. From 1989 to 2004, he shifted and promoted to a Lecturer and an Associate Professor with the School of Mechatronic Engineering, China University of Mining and Technology, where he was a Professor in 2005. Since 2011, he has been the Dean of the School of Mechatronic Engineering with the China University of Mining and Technology. His research interests include structure design of shearer, mobile target collaboration positioning, metro stray current monitoring, optical fiber sensing, and network architecture.

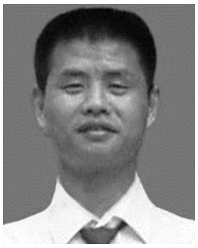

XUEFENG YANG was born in 1979. He received the B.E., M.E., and Ph.D. degrees from the School of Mechatronic Engineering, China University of Mining and Technology, Xuzhou, China, in 2004, 2006, and 2009, respectively. He is with the China University of Mining and Technology as an Associate Professor. His current research interests include shearer dynamics, robot dynamics, intelligent detection and information processing and design and application of micro-electromechanical system.

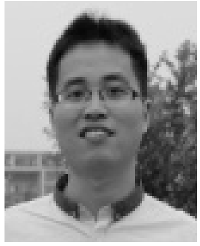

SHAOYI XU was born in 1988. He received the B.E., M.E., and Ph.D. degrees from the School of Mechatronic Engineering, China University of Mining and Technology, Xuzhou, China, in 2010, 2012, and 2015, respectively. He is with the China University of Mining and Technology as an Associate Professor. His current research interests include shearer dynamics, intelligent control of electro-mechanical system, and design and application of micro-electromechanical system.